DFNE 18–960

Discrete Element Modelling of Hydraulic Fracture Interaction with Natural Fractures in Shale Formations

Yildirim, B., Cao, W., Shi J-Q., Durucan, S., Korre, A.

Department of Earth Science and Engineering, Royal School of Mines, Imperial College London, London SW7 2AZ, United Kingdom

ABSTRACT: Research presented in this paper aimed at establishing a better understanding of natural fracture (NF)/hydraulic fracture (HF) interaction mechanisms and fracture network development in naturally fractured and nonhomogeneous shale formations through numerical modelling using the two-dimensional particle flow code (PFC2D). Hydraulic fracture propagation was firstly modelled in a 30 m x 30 m model representing intact rock by bonded particle method (BPM), which served as a base case in the research. Then a single, deterministic natural fracture was embedded into the same model by a smooth joint contact model (SJM) to investigate different NF/HF interaction mechanisms under a range of different conditions by varying the angle of approach, differential horizontal stress, and the mechanical properties of a fracture within the model. Based on the parametric research findings, number and diversity of natural fractures in the model were increased both deterministically and stochastically, and the results are compared and discussed.

1. INTRODUCTION

Economic development of low permeability shale gas reservoirs depends on the effectiveness of hydraulic fracturing operations, which aim at enhancing the permeability of the rock and increasing gas production through the developed fracture network. Therefore, an understanding of the mechanisms and field properties controlling hydraulic fracture propagation and fracture network development forms an important part of a successful hydraulic fracture design in naturally fractured reservoirs.

Numerical modelling of hydraulic fracture propagation in discontinuous rock masses is a complex and a multitask problem. Besides several complex reservoir rock conditions, such as low permeability, anisotropy, heterogeneity, geomechanical sensitivity, and different fluid flow mechanisms, which are characteristics of unconventional reservoirs, the ubiquity of natural discontinuities increase the complexity of hydraulic fracturing process in shale reservoirs. Most numerical modelling research on hydraulic fracturing process has been conducted based on continuum mechanics by adapting linear elastic fracture mechanics and bi-wing and symmetrical fracture propagation, however, ubiquity of natural discontinuities makes applicability of these assumptions questionable in heterogeneous and anisotropic unconventional reservoirs. Moreover, difficulties in exact representation of the progressive deformation in rock masses by continuum mechanics creates the need for more accurate numerical modelling approach. In this context, application of discontinuum mechanics in hydraulic fracture modelling has attracted attention in the past few decades, thanks to its capability and convenience in representing displacements, separation, slippage and automatic identification of contacts during rock fracturing and fluid injection processes (Kawamoto and Aydan, 1999; Bruno et al., 2001; Damjanac et al., 2010; Lisjak and Graselli, 2014).

Despite a significant number of numerical modelling studies being carried out on fracture network development in naturally fractured reservoirs, the combined role of different sets of natural fractures on NF/HF interaction mechanisms is still not well understood. To this end, this research aimed at developing a better understanding of NF/HF interaction and its impact on hydraulic fracture propagation by using discrete element modelling approach. In this context, this paper presents the numerical model results obtained by using both deterministic and stochastic discrete fracture network (DFN) approaches in two-dimensional Particle Flow Code (PFC2D). Firstly, the applicability of smooth joint contact model was demonstrated by evaluating different NF/HF interaction mechanisms under different conditions of angle of approach, differential stress, and the mechanical properties of a single fracture. The results were found to be consistent with the previous research findings in the literature (Blanton, 1982; Warpinski and

Teufel, 1987; Zhao and Young, 2009; Chuprakov et al., 2010; Chuprakov et al., 2013; Wu and Olson, 2014; Zhang et al., 2014, Huang et al., 2015; Yoon et al., 2017; Zhou et al, 2017). Next, diversity of natural fractures was increased by introducing deterministic or stochastic discrete fractures into the model. Model results are presented, and advantages and disadvantages of both techniques are discussed in the framework of fracture network modelling in PFC2D.

2. MODELLING METHODOLOGY

2.1. Model Set-up

A 30m×30m reservoir model was developed in PFC2D (Fig. 1). Particle radius was selected in the range 0.10-0.15 m and the model properties were assigned based on the mechanical and elastic properties of the shale samples, which were collected from the Hope Cement Works shale quarry in Derbyshire, UK and used for the experimental research carried out in the laboratory. Maximum horizontal (σ_H) and minimum horizontal stress (σ_h) magnitudes were set by the servo-control loading scheme implemented via the Fish function.

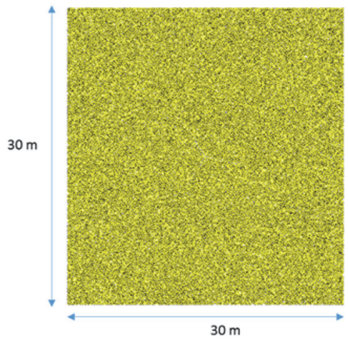

Fig. 1. The two-dimensional model configuration.

2.2. Choice of the Contact-stiffness and Contact-bond Models

The two-dimensional particle flow code represents the rock material as an assembly of round particles that are connected with breakable bonds with specific strength values. Particles interact with each other and with the walls, and these interactions between ball-to-ball and ball-to-wall cause a force to develop between these entities, which is referred to as 'contact'. There are two stiffness models available in PFC2D, which are the *linear model* and *simplified Hertz-Mindlin model*. In this research, the linear model was used in which the forces and relative displacements are linearly related by the constant contact stiffness. The bond models that model the brittleness of ball-to-ball bonds in PFC2D are classified under three groups as *contact bond*, *parallel bond* and *flat joint models*. In this research, flat-joint model was preferred due to its superiority in yielding more realistic compressive/tensile strength ratios as well as the friction angles for the rocks.

2.3. Assignment of the Material Properties

Particle-based discontinuum modelling techniques requires careful selection of micro parameters (Young's modulus, Poisson's ratio, cohesion and tensile strength) in order to yield the corresponding macro properties which are representative of field behaviour. Calibration process in PFC2D requires a trial and error procedure in which micro properties are modified until representative values of macro properties are obtained numerically.

The micromechanical input parameters were calibrated using the mechanical and elastic properties of the Derbyshire shale, which were determined in the laboratory. The calibration process was performed on a 5 × 10 cm synthetic model by conducting unconfined compressive strength (UCS) and direct tensile strength experiments on a bonded sample (Table 1).

Table 1. DEM calibration results

Parameter	Laboratory Data	DEM Results
Young's Modulus, E_c (GPa)	15.60	15.45
Poisson's Ratio	0.286	0.286
Internal Friction Angle, Φ (°)	31.00	31.00
UCS (MPa)	82.00	82.92
Tensile Strength, σ_t (MPa)	8.99	8.73

2.4. Fluid flow modelling

Fluid network modelling in PFC2D comprises "particles" and "fluid domains" that are enclosed by a chain of particles, and "pipes" as flow channels between the fluid domains.

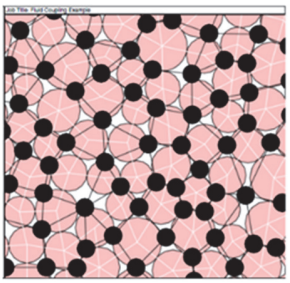

Fig. 2. Representation of domains (black dots), flow paths (black lines), and bonds (white lines) in compacted bonded assembly of particles (after PFC2D Version 4.0 Manual, 2008).

Fluid flow in the PFC model is simulated based on the Navier-Stokes equation as:

$$q = \frac{ka^3(P_2 - P_1)}{L} \quad (1)$$

where q is flow rate, k is a connectivity factor, a is aperture of the pipe, (P_2 - P_1) is the pressure difference between the two adjacent domains, and L is the length of

the pipe, which is taken as sum of the radii of the particles adjacent to the contact in question.

2.5. Fluid Flow and Geomechanical Coupling

Coupling of fluid flow and mechanical deformation plays an important role in the simulation of hydraulic fracturing of weak formations. Fluid pressure applies an extra force on particles, which affects the movement of particles. On the other hand, movement of particles may also lead to deformation of the domains and cause a change in pore pressure. Previous research by Yoon et al. (2014) indicated that the effect of mechanical change on domain pressure is not significant, therefore, one-way coupling approach, where fluid pressure has an effect on displacements, but not vice versa, was adopted in the study presented here.

2.6. Implementation of Natural Fractures

Due to explicit representation of joints, mechanical behaviour of jointed rock is well captured by the discrete element method (DEM) where rock discontinuities are represented by the smooth-joint contact model. All contacts between particles that are located on opposite sides of the joint are assigned as smooth-joint contacts. Particle pairs that are joined by smooth-joint contacts may overlap and slide past each other (Mas Ivars et al., 2008). Joint properties (friction angle, cohesion, dilation angle, tensile strength, as well as joint normal and shear stiffnesses) are conventionally obtained from laboratory experiments (PFC2D Version 4.0 Manual, 2008).

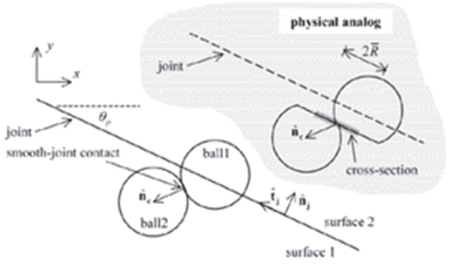

Fig. 3. Representation of smooth-joint contact in PFC2D (after PFC2D Version 4.0 Manual, 2008).

In this research, both deterministic and stochastic discrete fractures were introduced into the model. In the early stages, a single natural fracture was implemented with dip angles (Θ) of 0, 30 °, 60 °, and 90°. Next, the differential horizontal stress ($\Delta\sigma_h$), normal to shear stiffness ratio (k_n/k_s), and the friction angle of the NF were varied. Finally, the number of deterministic discrete fractures with the same mechanical and geometrical properties was increased to 2, 4, and 8 respectively and the fracture propagation paths in each case were analysed accordingly. Micro properties for smooth joint contacts were mainly derived from the published data (Bruner and Smosna, 2011; Gale et al., 2007; Lambert and Coll, 2014; Dinc et al., 2016; Ye et al., 2016; Hu et al., 2017).

In the second part of the research, two main natural fracture sets, DFN1 and DFN2 were implemented in the model stochastically. Joint set DFN1 represents sub horizontal fractures whereas DFN2 represents the sub-vertical ones. Fracture orientations were mainly derived from the orthogonal joint sets observed in the shale quarry (Fig. 4).

Fig. 4. The Derbyshire shale quarry joint sets.

Table 2. Smooth joint contact properties.

Parameter	Natural Fractures
Normal stiffness, k_n (GPa/m)	100
Shear stiffness (GPa/m)	10
Sj_ friction coefficient	0.15
Sj_ cohesion, c (MPa)	0
Tensile Strength, σ_t (MPa)	0
Aperture (m)	0.004
Size (m)	8

Mechanical properties presented in Table 2 were assigned to the smooth joint contacts around each fracture in the stochastic fracture model. Other than the mechanical properties, fracture size, fracture orientation, and fracture density/intensity were specified as the three main parameters in the assignment of randomly distributed stochastic discrete fractures. For the fracture size range, which varied between L_1= 5 m and L_2 = 10 m, a 4th degree power law distribution was used. On the other hand, fracture orientation both for sub-horizontal (Θ =5-10°) and sub-vertical fractures (Θ =75-90°) obeys uniform statistical distribution in the model. Fracture intensity (P_{10}), which is defined as the number of fractures per length of scan line, was used as 0.5 for both the natural fracture sets DFN1 and DFN2.

3. MODEL RESULTS

3.1. Hydraulic Fracture Interaction with Deterministic Discrete Fracture Networks

In this part of the research, different scenarios were simulated in order to gain further insights into effects of the angle of approach, Θ (Fig. 5), differential horizontal

stress, $\Delta\sigma_h$ (Fig. 6), stiffness ratio, k_n/k_s (Fig. 7) and friction coefficient, μ (Fig. 8) of the fracture, as well as ubiquity of deterministic fractures (Fig. 9) on NF/HF interaction. A detailed summary of all the scenarios and the resulting NF/HF interaction mechanisms are presented in Table 3.

Based on these results, the differential horizontal stress (σ_{hmax}-σ_{hmin}) was found to be the controlling factor in HF growth. Large differential stresses resulted in planar fracture growth with crossing mechanism while limited fracture growth was observed under low differential stress values. On the other hand, steeper angle of approach (60, 90°) was found to be favouring direct crossing whereas lower angles of approach (0, 30°) resulted in limited and diverted HF growth. Normal stiffness to shear stiffness ratio (k_n/k_s), which is a micromechanical parameter defined in the model both for the fracture (1.2, 2, 5, and 10) and for the intact rock matrix (3.4), was found to be another important parameter affecting the HF growth and thus the HF/NF interaction mechanism. It was observed that, when the stiffness ratio of the fracture is lower than that of intact rock matrix, branching in fracture propagation with arrest mechanism occurs, while higher stiffness ratios for the fracture results in planar fracture growth with crossing mechanism. It was also observed that crossing becomes favourable when friction angle (μ) of the fracture approaches to that of the intact rock matrix. Finally, an increase in the number of NFs resulted in different NF/HF mechanisms (direct crossing and dilation of NF).

Table 3. Different HF/NF interaction mechanisms for the scenarios presented in Figures 5, 6, 7, 8 and 9.

Scenario	HF growth and NF/HF interaction mechanism.
(a) Intact rock-reference case	Planar growth.
(b) Single fracture, $\Theta = 0^o$	Limited growth along the NF.
(c) Single fracture, $\Theta = 30^o$	Planar growth and no NF/HF interaction, diverted in the HF growth path.
(d) Single fracture, $\Theta = 60^o$	Planar growth and NF/HF interaction with cross mechanism.
(e) Single fracture, $\Theta = 90^o$	Planar growth and NF/HF interaction with direct cross mechanism.
(f) σ_{Hmax}=30MPa, σ_{hmin}=25MPa	Limited growth, no NF/HF interaction.
(g) σ_{Hmax}=30MPa, σ_{hmin}=20MPa	Planar growth and NF/HF interaction with cross mechanism.
(h) σ_{Hmax} = 30MPa, σ_{hmin} = 15MPa	Planar growth and NF/HF interaction with cross mechanism.
(i) σ_{Hmax} = 30MPa, σ_{hmin} = 10MPa	Planar growth and NF/HF interaction with cross mechanism.
(j) Single fracture, k_n= 12 GPa, k_s = 10 GPa	Branching in HF growth and NF/HF interaction with arrest mechanism.
(k) Single fracture, k_n= 20 GPa, k_s = 10 GPa	Branching in HF growth and NF/HF interaction with arrest mechanism.
(l) Single fracture, k_n= 50 GPa, k_s = 10 GPa	Planar growth and NF/HF interaction with cross mechanism.
(m) Single fracture, k_n= 100 GPa, k_s = 10 GPa	Planar growth and NF/HF interaction with cross mechanism.
(n) Single fracture, μ = 0.15	Planar growth and NF/HF interaction with cross mechanism.
(o) Single fracture, μ = 0.3	Planar growth and NF/HF interaction with cross mechanism.
(p) Single fracture, μ = 0.6	Planar growth and NF/HF interaction with direct cross mechanism.
(r) Single fracture, μ = 0.8	Planar growth and NF/HF interaction with direct cross mechanism.
(s)Two parallel fractures, $\Theta = 90^o$	Planar growth and NF/HF interactions with direct cross mechanism in one side, arrest mechanism in another side.
(t) 2 Orthogonal fracture sets, Θ_1= 0 and $\Theta_2 = 90^o$	Planar growth and NF/HF interactions with direct cross mechanism in one side, arrest mechanism in another side.
(u) 2 Orthogonal fracture sets, Θ_1= 0 and $\Theta_2 = 90^o$	Complex fracture growth and NF/HF interaction with arrest mechanism in two sides and cross mechanism in one side.

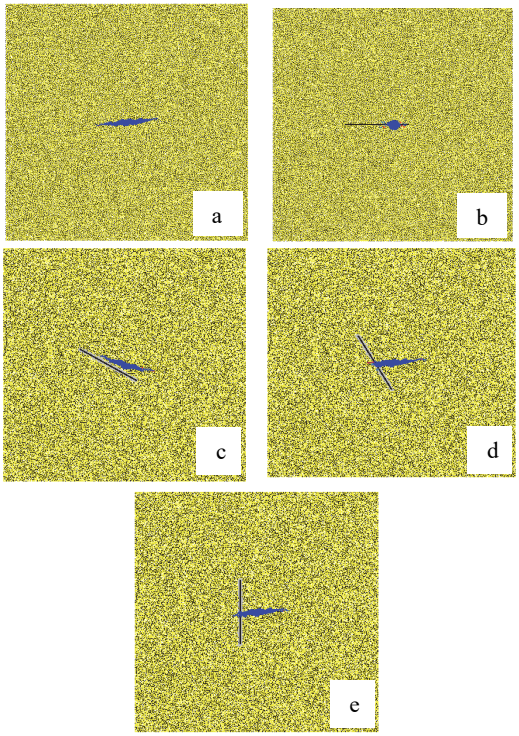

Fig. 5. The effect of the angle of approach (Θ) on NF/HF interaction.

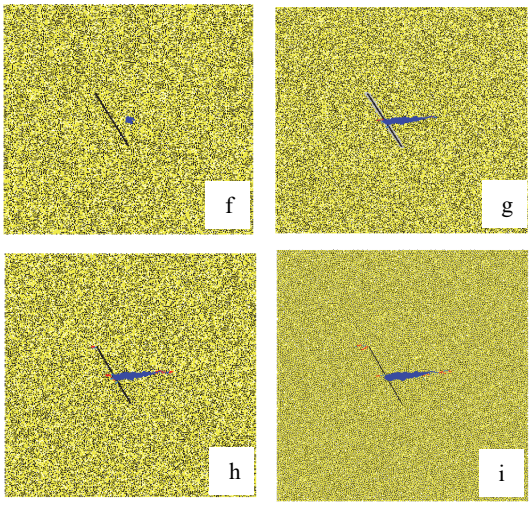

Fig. 6. The effect of differential horizontal stress ($\Delta\sigma_h$) on NF/HF interaction.

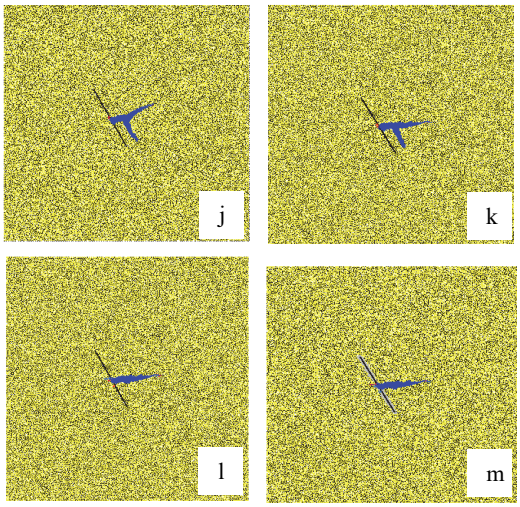

Fig. 7. The effect of fracture stiffness ratio (k_n/k_s) on NF/HF interaction.

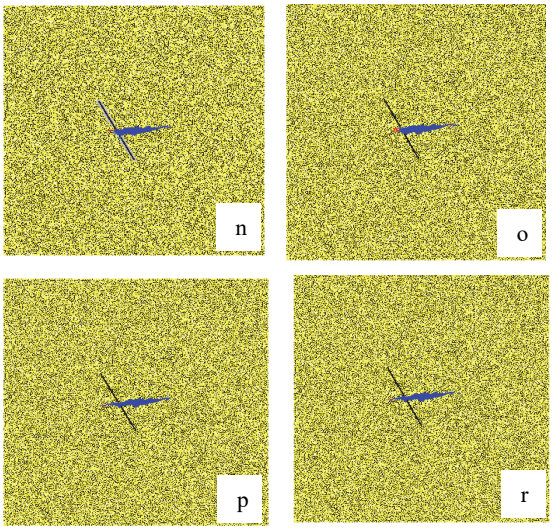

Fig. 8. The effect of fracture friction coefficient (μ) on NF/HF interaction.

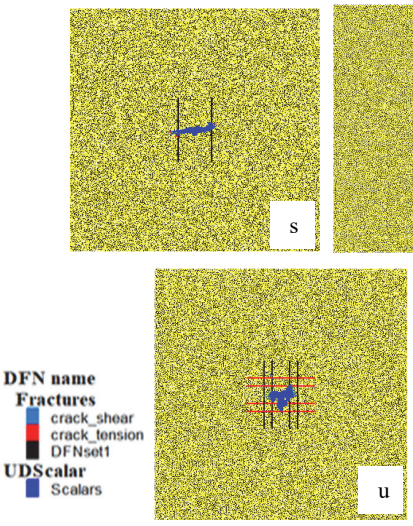

Fig. 9. The effect of increased number of NFs on NF/HF interaction.

3.2. *Hydraulic Fracture Interaction with Stochastic Discrete Fracture Networks*

Figure 11 presents the results of NF/HF interactions for 5 stochastically generated discrete fracture networks using the same model described in Section 2.6.

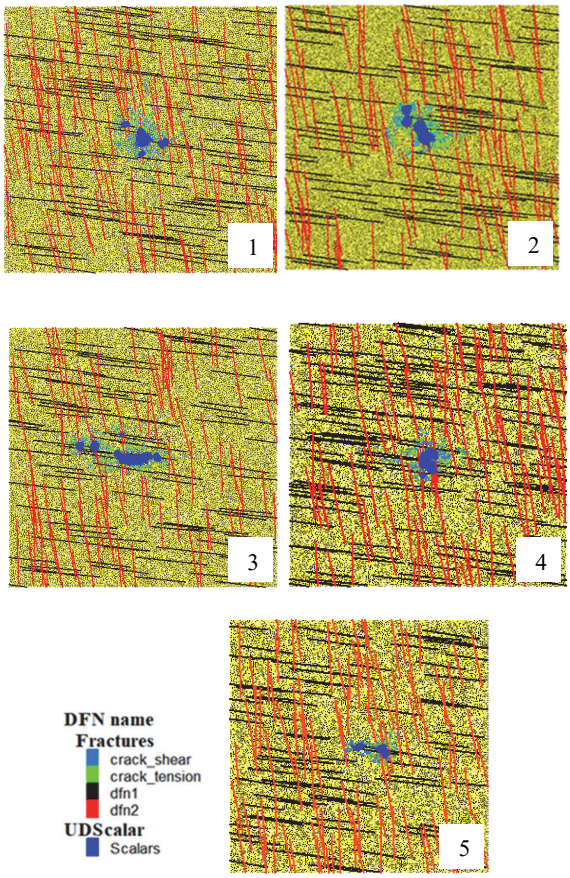

Fig. 10. NF/HF interaction for stochastically generated discrete fracture realisations.

It is observed from Fig. 10 that ubiquity of natural fractures led to more complex fracture propagation with increased number of tensile and shear cracks, compared with a simple and planar fracture growth in the above deterministic DFN models. Moreover, HF propagated along the nearest NF instead of being favoured by the in-situ stress state as was the case in the deterministic DFN model. On the other hand, stiffness ratio (k_n/k_s) of the fracture is also found to be a significant parameter affecting the complexity of HF growth.

4. CONCLUSIONS

In the research described here, deterministic DFN models were first used to investigate different NF/HF interaction mechanisms by varying the angle of approach, differential horizontal stress, and mechanical properties of the NFs. Both direct crossing (with and without penetration) and arresting mechanisms were observed, and the differential stress was found to be the controlling factor in HF growth. Use of stochastically generated NFs in the model, which are believed to be more representative of the field conditions, have shown that the HF propagation and NF/HF interaction is mainly affected by the ubiquity of the natural fractures. Future work aims at extending the design and analysis of stochastic DFN models towards the assessment of hydraulic fracture connectivity through correlation with models of laboratory hydrofracturing experiments.

ACKNOWLEDGEMENTS

The first author wishes to thank the Schlumberger Faculty for the Future Fellowship for the support she receives towards her research at Imperial College. The second author acknowledges the UK Engineering and Physical Sciences Research Council (EPSRC) scholarship awarded by the Faculty of Engineering at Imperial College London.

REFERENCES

Blanton, T. L. 1982. An experimental study of interaction between hydraulically induced and pre-existing fractures. SPE/DOE In *Unconventional Gas Recovery Symposium, 16-18 May, Pittsburgh, PA.*

Bruner, K. R., and R. Smosna. 2011. A comparative study of the Mississippian Barnett Shale, Fort Worth Basin, and Devonian Marcellus Shale, Appalachian Basin. In *US DOE Report*: 118.

Bruno, M.S., A. Dorfmann, K. Lao, and C. Honeger. 2001. Coupled particle and fluid flow modelling of fracture and slurry injection in weakly consolidated granular media. *ARMA, 38th U.S. Symposium on Rock Mechanics, 7-10 July, Washington, D.C.*

Chuprakov, D.A., A. V. Akulich, E. Siebrits, and M. Thiercelin. 2010. Hydraulic fracture propagation in a naturally fractured reservoir. In *SPE Oil and Gas India Conference and Exhibition, 20-22 January, Mumbai*.

Chuprakov, D.A., O. Melcheava, and R. Prioul. 2013. Hydraulic Fracture propagation across a weak discontinuity controlled by fluid injection. In *Effective and Sustainable Hydraulic Fracturing*, ed. Andrew P. Bunger, John McLennan and Rob Jeffrey.

Damjanac, B., I. Gil, M. Pierce, and M. Sanchez. 2010. A new approach to hydraulic fracturing modeling in naturally fractured reservoirs. In *44th US Rock Mechanics Symposium and 5th US Canada Rock Mechanics Symposium*, *Salt Lake City, UT.*

Dinc, O., and Z. Karaca. 2017. The effects of strength parameters on failure mechanisms in weak rocks. In *EUROROCK,* August 2016.

Gale, J. F. W, R. M. Reed, and J. Holder. 2007. Natural fractures in the Barnett Shale and their importance for hydraulic fracture treatments, *AAPG Bulletin*, 91: 603-622.

Huang, J., R. Safari, U. Mutlu, K. Burns, I. Geldmacher, M. McClure, and S. Jackson. 2015. Natural-hydraulic fracture interaction: Microseismic observations and geomechanical predictions. In *Unconventional Resources Technology Conference, Denver, 25-27 August.*

Hu, W., C. Y. Kwok, K. Duan, and T. Wang. 2017. Parametric study of the smooth-joint contact model on the mechanical behavior of jointed rock: *International Journal for Numerical and Analytical Methods in Geomechanic*s: 1–19.

Kawamoto, T., and Ö. Aydan. 1999. A review of numerical analysis of tunnels in discontinuous rock masses: *International Journal for Numerical and Analytical Methods in Geomechanics*. 23(13): 1377–1391.

Lambert C, and C. Coll, 2014. Discrete modeling of rock joints with a smooth-joint contact model. *J Rock Mech Geotech Eng 2014, 6 : 1–12.*

Lisjak, A., and G. Graselli. A review of discrete modeling techniques for fracturing processes in discontinuous rock masses. *Journal of Rock Mechanics and Geotechnical Engineering.* 2014. 6: 301-314.

Mas Ivars D., D. O. Potyondy, M. Pierce and P. A. Cundall, 2008. The smooth-joint contact model. In *5th European Congress on Computational Methods in Applied Sciences and Engineering, Venice*, *30 June -5 July.*

PFC2D Version 4.0 Manual, 2008.

Warpinski, N. R, and L. W. Teufel. 1987. Influence of geologic discontinuities on hydraulic fracture propagation. *Journal of Petroleum Technology.* 39 (2): 209-220.

Wu, K. and J. E. Olson. 2014. Mechanics analysis of interaction between hydraulic and natural fractures in shale reservoirs. In *URTEC Conference, Denver, Colorado, USA*.

Ye, Z., A. Ghassemi, and S. Riley. 2016. Fracture properties characterization of shale rocks. *SPE Journal*. 2: 1–13.

Yoon, J. S., A. Zang, O. Stephansson. 2014. Numerical investigation on optimized stimulation of intact and naturally fractured deep geothermal reservoirs using hydro-mechanical coupled discrete particles joints model. *Geothermics.* 52:165:184.

Yoon, J.S., A. Zang, O. Stephansson, H. Hofmann, and G. Zimmermann. 2017. Discrete element modelling of hydraulic fracture propagation and dynamic interaction with natural fractures in hard rock. *Procedia Engineering*. 191: 1023 – 1031.

Zhang, F., N. Nagel, and F. Sheibani. 2014. Evaluation of hydraulic fractures crossing natural fractures at high angles using a hybrid discrete- continuum model. In *ARMA, 48th U.S. Rock Mech/Geomechanics Symposium*, *Minnesota, 1-4 June.*

Zhao, X. P. and R.P. Young. 2009. Numerical simulation of seismicity induced by hydraulic fracturing in naturally fractured reservoirs. In *SPE Annual Technical Conference and Exhibition, 4-7 October, New Orleans, Louisiana*.

Zhou, J., L. Zhang, Z. Pan, and H. Zhenhua. 2017. Numerical studies of interactions between hydraulic and natural fractures by smooth joint model. *Journal of Natural Gas Science and Engineering*. 46: 592-602.